Failure resistance of amorphous silicon transistors under extreme in-plane strain

H. Gleskova[a)] and S. Wagner
Department of Electrical Engineering, Princeton University, Princeton, New Jersey 08544

Z. Suo
Department of Mechanical and Aerospace Engineering and Princeton Materials Institute, Princeton University, Princeton, New Jersey 08544

(Received 26 July 1999; accepted for publication 8 September 1999)

We have applied strain on thin-film transistors (TFTs) made of hydrogenated amorphous silicon on polyimide foil. In tension, the amorphous layers of the TFT fail by periodic cracks at a strain of ~0.5%. In compression, the TFTs do not fail when strained by up to 2%, which is the highest value we can set controllably. The amorphous transistor materials can support such large strains because they lack a mechanism for dislocation motion. While the *tensile* driving force is sufficient to overcome the resistance to crack formation, the *compressive* failure mechanism of delamination is not activated because of the large delamination length required between transistor layers and polymer substrate. © *1999 American Institute of Physics.* [S0003-6951(99)01745-3]

Much of the recent research on thin-film electronics has been focused on the fabrication of devices on plastic substrates[1–8] for applications that require nonbreakable or flexible substrates. In traditional electronics thin films are deposited on substrates that are *stiff* and thick, so that the films must conform to the substrate. Most of any stress that develops is concentrated in the film, and the substrate remains nearly free of stress. However, when the substrate becomes *compliant* and thin, it can take up significant stress and thereby reduce the stress in the film.[9] Young's moduli Y_f of the hydrogenated amorphous silicon (a-Si:H) materials and the metals used in thin-film transistors (TFTs) are ~ 200 GPa,[10–13] while Y_s of the polyimide Kapton E substrate is ~ 5 GPa.[14] The thickness d_f of the TFT structure typically is $\sim 1\ \mu$m so that the compliant condition is established for a Kapton thickness of $d_s \lesssim 300\ \mu$m.[9]

Theory predicts that a compliant substrate should allow the bending of thin-film transistors to very small radii of curvature.[9] When we sought to verify this prediction experimentally, we made the surprising discovery that the TFTs do not fail at all under the highest compressive strain that we can establish accurately. This letter reports our experimental observations and their brief theoretical analysis.

All TFT silicon layers were deposited on 25 μm thick Kapton E foil at 150 °C[2] using a three-chamber rf-excited plasma enhanced chemical vapor deposition system. The TFTs have the bottom gate, back-channel etch structure shown in Fig. 1. Arrays of TFTs with gate length $L = 15\ \mu$m and width $W = 210\ \mu$m were fabricated on 38 mm×38 mm substrates. The fabrication is described elsewhere.[2] The TFTs were made on Kapton foil coated on both faces with a layer of SiN_x as shown in Fig. 1(a). This structure corresponds to a stiff substrate. The backside layer of SiN_x was removed from part of the samples to convert the substrate to compliant, as shown in Fig. 1(b).

The as-fabricated TFT/substrate structures [Fig. 1(a)] had built-in radii of curvature R_0 of 18 mm, with the TFTs on the outside, and the compliant structures [Fig. 1(b)] $R_0 = 8$ mm, with the TFTs still on the outside.

We calculate the strain produced in the channel of the TFT by forced bending. The substrate with d_s and Y_s is covered on one or both sides with stiff films with Y_f and d_{f1} and d_{f2} [Fig. 2(a)]. During bending the outside film is under tension while the one on the inside is under compression. The strain $\epsilon_{\rm surface}$ on the surface of the TFT film bent to a radius of curvature R is[15]

$$\epsilon_{\rm surface}=\left(\frac{1}{R}\pm\frac{1}{R_0}\right)\frac{d_s+d_{f1}+d_{f2}}{2} \cdot\frac{\chi(\eta_1^2+\eta_2^2)+2(\chi\eta_1+\chi\eta_1\eta_2+\eta_2)+1}{\chi(\eta_1+\eta_2)^2+(\eta_1+\eta_2)(1+\chi)+1}, \quad (1)$$

where $\chi = Y_f/Y_s$, $\eta_1 = d_{f1}/d_s$, and $\eta_2 = d_{f2}/d_s$. The plus or minus signs are for bending opposite to or with the built-in curvature. Figure 3 shows the bending strain from Eq. (1), for the stiff [Fig. 1(a)] and the compliant [Fig. 1(b)]

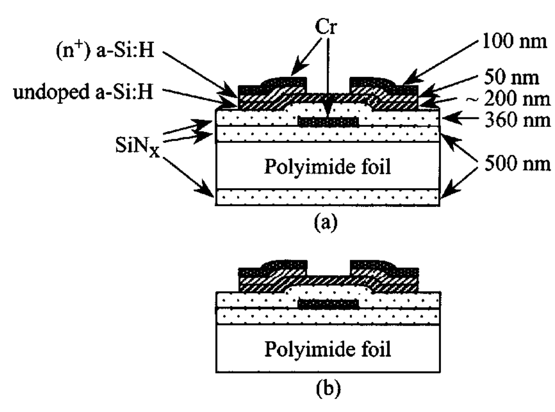

FIG. 1. Cross section of a-Si:H TFT on 25 μm thick Kapton foil: (a) stiff substrate—the as-fabricated sandwich structure; (b) compliant substrate—back SiN_x removed.

[a)]Electronic mail: gleskova@ee.princeton.edu

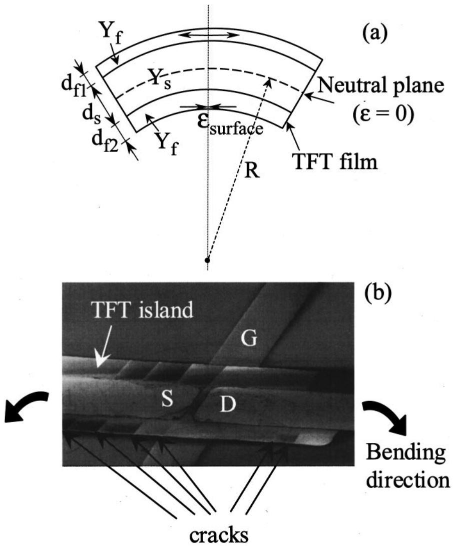

FIG. 2. (a) Films-on-foil structure bent to a cylindrical roll. (b) SEM picture of a failed TFT after outward bending. The TFT failed at $R = 2$ mm.

structures. One can clearly see that removing the back SiN_x layer reduces the strain in the TFT channel area by a factor of ~ 2.

We stressed individual transistors on Kapton substrates mechanically by bending outward [top surface of Fig. 2(a)] or inward [bottom surface of Fig. 2 (a)]. Single TFTs were bent to decreasing R, beginning with $R = 4$ mm down to $R = 0.5$ mm. The TFT was stressed for 1 min at each bending radius, and then was released, flattened and remeasured. Figure 4 summarizes the effects of inward/compressive (a),(c) and outward/tensile (b),(d) bending on TFT performance. The top graphs in each subset show the on-current I_{on}, the off-current I_{off}, and the gate-leakage current I_{leak} as functions of the radius of curvature. Likewise, the bottom graphs in each subset show the threshold voltage V_T and the saturated electron mobility μ_n, calculated from the transfer characteristic at source-drain voltage $V_{ds} = 10$ V. Differences between the ''initial'' characteristics reflect spread between as-fabricated TFTs.

Inward/compressive bending (left column of Fig. 4) leaves I_{on}, I_{off}, I_{leak}, and μ_n virtually unchanged, regardless of compliant or stiff substrate. The slight monotonous rise in V_T is electrical drift also observed in repeated measurements of unstressed TFTs. This result shows that the TFT can be compressed by at least 2% without failing.

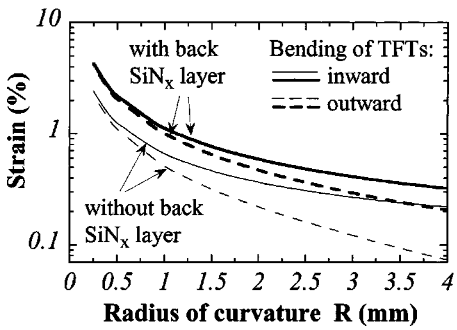

FIG. 3. Inward and outward bending strain in the channel area of the TFT as a function of radius of curvature, calculated from Eq. (1) [$d_s = 25\ \mu$m, $Y_s = 5$ GPa, $Y_f = 183$ GPa (Ref. 11), $d_{f1} = 500$ nm, and $d_{f2} = 960$ nm].

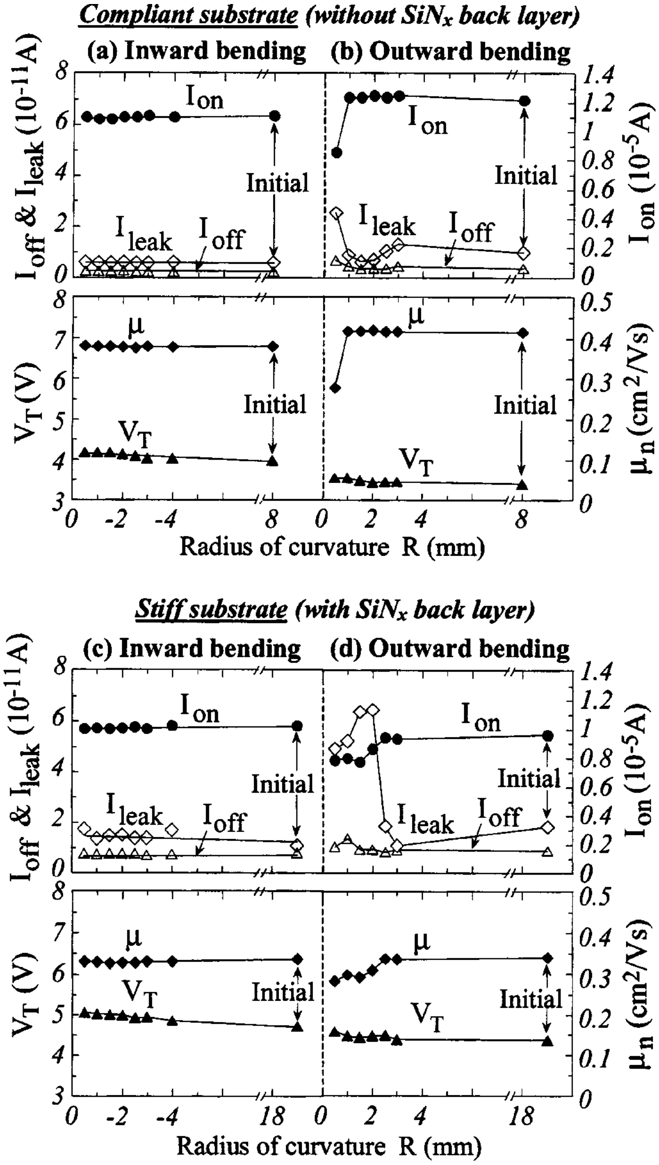

FIG. 4. On-, source-gate leakage, off-currents, electron mobility, and threshold voltage in the saturation regime as functions of bending radius. I_{off} is the smallest source–drain current at $V_{ds} = 10$ V, I_{on} is the source–drain current for $V_{ds} = 10$ V and the gate voltage $V_{gs} = 20$ V, and I_{leak} is the source–gate current for $V_{ds} = 10$ V and $V_{gs} = 20$ V. Outward bending R is defined positive, inward bending negative. Differences between the initial characteristics reflect spread between as-fabricated TFTs.

Outward/tensile bending (right column of Fig. 4) produces electrical effects at larger values of R on the stiff substrate [Fig. 4(d)] than on the compliant substrate [Fig. 4(b)], as expected from Fig. 3. No substantial changes are observed down to $R = 1$ mm (0.5% strain) on the compliant substrate and $R = 2.5$ mm (0.4% strain) on the stiff substrate. Several TFTs on stiff substrates failed at $R \sim 2$ mm. The electrical failure resulted from periodic cracks in the TFT island that run perpendicular to the bending direction [see Fig. 2(b)]. For strains $\gtrsim 0.5\%$ about 50% of the TFTs still functioned with a deteriorated electrical performance.

The amorphous material cannot release strain by dislocation motion, and therefore deforms elastically until it cracks. Under tension the crack originates at a flaw and propagates as long as the driving force G is larger than the crack resistance, which is given by the surface energy of the newly formed crack Γ_f:

$$G \equiv \beta \frac{(1-\nu_f^2)\sigma_f^2 d_f}{Y_f} > \Gamma_f. \quad (2)$$

Here σ_f is the stress in the film, ν_f is the film's Poisson ratio, and β is a dimensionless number that depends on the elastic constants of the film and the substrate.[16] When the substrate is compliant β becomes much larger than unity, and the crack propagates easily.

Under compression the film may delaminate from the substrate[16] after the film has buckled. Buckling requires a large enough area of unbonded film, i.e., a defective film/substrate interface. After buckling, both normal and shear stresses develop on the interface at the buckle front, which may motivate the unbonded area to grow like a crack. The critical unbonded length for buckling l_c is given by

$$l_c = \frac{\pi d_f}{\sqrt{3(1-\nu_f^2)}} \left(-\frac{Y_f}{\sigma_f} \right)^{1/2}. \quad (3)$$

This expression comes from Euler's solution of a buckling column, adjusted for the plane strain condition. It applies to an unbonded area of any shape, if a shape-dependent dimensionless coefficient is included. Figures 3 and 4 show that $-\sigma_f/Y_f = \epsilon_f \geqslant 0.02$, which gives $l_c \leqslant 10 d_f \sim 10\ \mu$m. Therefore, the TFT structure is very stable under compression, because failure requires a preexisting unbonded area that may have to be as large as 10 μm.

In earlier reports, TFTs fabricated on glass changed at much lower bending strain,[17] but among the experiments on the bending of single a-Si:H layers deposited on glass or Kapton substrates,[18–21] Ref. 19 suggests a failure strain comparable to ours. Converting the maximum applied tensile or compressive stress of 3 GPa[19] with $Y(a\text{-Si:H}) = 150$ GPa,[10] we calculate that the a-Si:H layer was subjected to a strain of $\sim 2\%$. However, strain data for single SiN_x layers, which we would need for a quantitative comparison, have not been reported.

Thus, when a-Si:H TFTs fabricated on steel[22] or Kapton are bent in tension, they function up to a strain of $\sim 0.5\%$. For higher strains the TFTs on steel delaminate, while about 50% of the TFTs on Kapton (stiff or compliant) still function with a deteriorated electrical performance. Compression produces TFT results that are different for steel and Kapton substrates. While the former delaminate at a strain of $\sim 0.5\%$, the latter function up to strain of at least 2%. The mechanical failure in compression is determined by the bonding between the substrate and the TFT structure. We expect that very high compressive strains can be reached with good bonding.

The authors gratefully acknowledge support from the DARPA HDS program and thank DuPont for donating Kapton E foils.

[1] G. N. Parsons, C. S. Yang, C. B. Arthur, T. M. Klein, and L. Smith, Mater. Res. Soc. Symp. Proc. **508**, 19 (1998).
[2] H. Gleskova, S. Wagner, and Z. Suo, Mater. Res. Soc. Symp. Proc. **508**, 73 (1998).
[3] J. N. Sandoe, Digest of Technical Papers of the Society for Information Display, 1998, Vol. 29, p. 293.
[4] E. Lueder, M. Muecke, and S. Polach, Proceedings of the International Display Research Conference, Asia Display '98, 1998, p. 173.
[5] A. Constant, S. G. Burns, H. Shanks, C. Gruber, A. Landin, D. Schmidt, C. Thielen, F. Olympie, T. Schumacher, and J. Cobbs, The Electrochemical Society Proceedings, 1995, Vol. 94-35, p. 392.
[6] S. G. Burns, H. Shanks, A. Constant, C. Gruber, D. Schmidt, A. Landin, and F. Olympie, The Electrochemical Society Proceedings, 1997, Vol. 96-23, p. 382.
[7] D. B. Thomasson, M. Bonse, J. R. Huang, C. R. Wronski, and T. N. Jackson, Tech. Dig. Int. Electron Devices Meet., p. 253 (1998).
[8] S. D. Theiss, P. G. Carey, P. M. Smith, P. Wickboldt, T. W. Sigmon, Y. J. Tung, and T.-J. King, Tech. Dig. Int. Electron Devices Meet., p. 257 (1998).
[9] Z. Suo, E. Y. Ma, H. Gleskova, and S. Wagner, Appl. Phys. Lett. **74**, 1177 (1999).
[10] M. D. Kluge and J. R. Ray, Phys. Rev. B **37**, 4132 (1988).
[11] F. Jansen and M. A. Machonkin, J. Vac. Sci. Technol. A **6**, 1696 (1988).
[12] T. S. Hickernell, F. M. Fliegel, and F. S. Hickernell, *IEEE Ultrasonic Symposium Proceedings* (IEEE, New York, 1990), p. 445.
[13] A. G. van Nie, Solid State Technol. **557**, 81 (1980).
[14] Kapton E, DuPont Films, P.O. Box 89, Circleville, OH 43113.
[15] H. Gleskova, S. Wagner, and Z. Suo, Mat. Res. Soc. Symp. Proc. (in press).
[16] J. W. Hutchinson and Z. Suo, Adv. Appl. Mech. **29**, 64 (1992).
[17] B. L. Jones, J. Non-Cryst. Solids **77&78**, 1405 (1985).
[18] M. Stutzmann, Appl. Phys. Lett. **47**, 21 (1985).
[19] S. Guha, W. den Boer, S. C. Agarwal, and M. Hack, Appl. Phys. Lett. **47**, 947 (1985).
[20] A. Ghaith, Philos. Mag. Lett. **55**, 197 (1987).
[21] M. Vaněček, J. Kočka, M. Nesládek, E. Šípek, O. Štika, and A. Tříska, Proceeding of the 7th E. C. Photovoltaic Solar Energy Conference, 1986, edited by A. Goetzberger, W. Palz, and G. Willeke, p. 402.
[22] E. Y. Ma and S. Wagner, Mater. Res. Soc. Symp. Proc. **508**, 13 (1998).